

5

Hepatic VLDL production in *ob/ob* mice is not stimulated by massive *de novo* lipogenesis but is less sensitive to the suppressive effects of insulin.

Coen H. Wiegman ^{*1}

Robert H.J. Bandsma ^{*1}

Margriet Ouwens ²

Fjodor H. van der Sluijs ¹

Rick Havinga ¹

Theo Boer ¹

Dirk-Jan Reijngoud ¹

Johannes A. Romijn ³

Folkert Kuipers ¹

¹ Groningen University Institute for Drug Exploration, Center for Liver,
Digestive and Metabolic Diseases, Department of Pediatrics,
University Hospital Groningen, Groningen, The Netherlands

² Department of Molecular Cell Biology, University Hospital Leiden,
Leiden, The Netherlands

³ Department of Endocrinology, University Hospital Leiden, Leiden

* Equally contributed to this work.

Abstract

Type 2 diabetes in humans is associated with increased *de novo* lipogenesis (DNL), increased fatty acid (FA)-fluxes, decreased FA oxidation and hepatic steatosis. In this condition, VLDL production is increased and resistant to suppressive effects of insulin. The relationships between hepatic FA metabolism, steatosis and VLDL production are incompletely understood. We investigated VLDL-triglyceride and apolipoprotein (apo)B production in relation to DNL and insulin sensitivity in female *ob/ob* mice. Hepatic triglyceride (5-fold) and cholesteryl ester (15-fold) contents were increased in *ob/ob* mice compared to lean controls. Hepatic DNL was increased ~10-fold in *ob/ob* mice whereas hepatic cholesterol synthesis was not affected. Basal rates of hepatic VLDL-triglyceride and apoB100 production were similar between the groups. Hyperinsulinemic clamping reduced VLDL-triglyceride and -apoB100 production rates by ~60 % and ~75 %, respectively, in lean mice but only by ~20 % and ~20 %, respectively, in *ob/ob* mice. No differences in hepatic expression of genes encoding apoB and microsomal triglyceride transfer protein were found. Hepatic expression and protein phosphorylation of insulin receptor and insulin receptor substrate-isoforms were reduced in *ob/ob* mice. Thus, strongly induced hepatic DNL is not associated with increased VLDL production in *ob/ob* mice, possibly related to differential hepatic zonation of apoB synthesis (periportal) and lipid accumulation (perivenous) and/or relatively low rates of cholesterogenesis. Insulin is unable to effectively suppress VLDL-triglyceride production in *ob/ob* mice, presumably due to impaired insulin signaling.

Introduction

Type 2 diabetes mellitus (DM2) is associated with increased *de novo* lipogenesis (DNL), decreased plasma fatty acid (FA) oxidation and an increased FA-flux from peripheral tissues to the liver.¹ These factors may all contribute to hepatic steatosis and increased hepatic VLDL production, two characteristic hallmarks of type 2 diabetes,² and are probably related to hepatic insulin resistance, i.e., an insensitivity of hepatic metabolic processes to the effects of insulin. The relative contribution of the various pathways in hepatic lipid metabolism to the development of a fatty liver and disturbances in VLDL production is unknown but may, at least in part, be related to the localization of these processes within the liver. Fatty acid synthesis and triglyceride (TG) accumulation occur predominantly in the perivenous areas (zone 3) of the liver whereas FA oxidation is more associated with the periportal areas (zone 1).^{3,4} VLDL secretion has so far not been restricted to a specific hepatic zone.

Leptin-deficient *ob/ob* mice develop a fatty liver, insulin resistance and hyperlipidemia.^{5,6} The contribution of hepatic lipoprotein production to the development of hyperlipidemia in these mice is not clear. Hyperglycemia together with an increased glycolytic activity in *ob/ob* mice may lead to an increased availability of acetylCoA residues for DNL,⁷ as supported by increased hepatic expression levels and activities of glycolytic enzymes, i.e., glucokinase,^{8,9} phosphofructokinase⁷ and pyruvate kinase.^{7,8} Furthermore, elevated plasma FFA levels⁹ and increased hepatic expression of fatty acid translocase (FAT or CD36) and plasma membrane-fatty acid binding protein (pmFABP) have been reported in this model.¹⁰ Increased endoplasmic reticulum (ER)-associated acetylCoA synthase (ACS) activity may increase the FA availability for esterification rather than for oxidation,¹⁰ which could contribute in increased TG and cholesteryl ester formation.

Insulin resistance seen in DM2 is associated with increased VLDL production.² Acute hyperinsulinemia reduces VLDL production in healthy volunteers^{11,12} but not in DM2 patients² and obese individuals.¹¹ Despite the insulin resistant condition and an increased hepatic TG content in *ob/ob* mice, a decreased VLDL-TG production rate under basal fasted conditions has been reported in this model.^{13,14} However, increased VLDL-TG secretion in *ob/ob* mice associated with enhanced expression and activity of the microsomal triglyceride transfer protein (MTP) has also been reported.¹⁵ The reason for these discrepant observations is unknown. The impact of insulin on VLDL production in the *ob/ob* mouse model has not been reported previously. Therefore, we quantified hepatic DNL and cholesterol synthesis using mass isotopomer distribution analysis (MIDA) and related the synthesis rates to VLDL-TG and -apoB production rates determined under basal conditions and during hyperinsulinemic clamps in *ob/ob* mice and in lean littermates. Hepatic insulin signaling and expression levels of genes encoding transcription factors and important enzymes involved in fatty acid and cholesterol metabolism, VLDL formation and insulin signaling, were studied to provide a mechanistic basis for our findings.

Methods

Animals

Female *ob/ob* and lean littermates were purchased from Harlan (Zeist, The Netherlands) and housed in a light- and temperature controlled facility. Experimental protocols were approved by the local Experimental Ethical Committee for Animal Experiments.

Analytical kits

Plasma and hepatic triglyceride (TG), cholesterol and glucose levels were determined by commercially available kits (Roche, Mannheim, Germany). Plasma and hepatic phospholipid concentrations and plasma free fatty acids (FFA) concentrations were determined with Phospholipid-kit and NEFA-C kit, respectively (Wako Chemical GmbH, Neuss, Germany). Plasma insulin was determined by a radio-immunoassay (RIA) RI-13K (Linco Research, Inc., St. Charles).

Experimental procedures

Female *ob/ob* and lean mice, weighing between 51-63 gram and 24-28 gram respectively, were *ad libitum* fed normal chow diet (RMH-B 2181, Hope Farms BV, Woerden, The Netherlands) enriched with 2 % [^{13}C]-acetate (Isotec, Miamisburg, OH). After 11 days, mice were fasted for 4 h, anaesthetized with halotane and livers were excised. A portion of abdominal fat was also collected. Liver and fat tissue were immediately frozen in liquid nitrogen and stored at -80°C . Blood was collected by heart puncture and immediately placed on ice in EDTA-containing tubes and centrifuged 10 minutes at 5,000 rpm at 4°C .

Hyperinsulinemic clamp

To study effects of insulin on lipoprotein metabolism, a second group of lean and *ob/ob* mice received a hyperinsulinemic clamp or a saline infusion under anesthesia after a 9 hour fast. Based on euglycemic insulin clamps performed in rats and mice by Hawkins and Rossetti *et al.*,^{16,17} in which insulin concentrations were fixed at ~ 25 ng/ml, we used a single infusate to establish hyperinsulinemia and euglycemia. The procedure was tested in pilot experiments. The infusate contained insulin (18 mU/kg/min; Novo Nordisk, Bagsvaerd, Denmark), somatostatin (1.5 $\mu\text{g}/\text{kg}/\text{min}$; UCB, Breda, The Netherlands) and glucose (25 mg/kg/hr; Merck, Darmstadt, Germany). All solutions were freshly prepared in saline containing 1.5 % BSA (Sigma, St. Louis, MO). Blood glucose concentration was determined with a GlucoTouch-glucose analyzer (LifeScan, Beerse, Belgium). The total infusion time was 2 hours. After 1 h mice received a Triton WR1339 injection (Sigma, St. Louis, MO) as a 12 % $^{\text{wt}}/\text{wt}$ solution dissolved in saline, in a dose of 5 ml/kg lean BW.¹⁹ Blood samples were taken before (t_0) and 30 and 60 minutes after Triton injection. At the end of the experiment a large blood sample was obtained by heart puncture for isolation of VLDL particles (see further). VLDL production rates were calculated from the slope of the linear TG *versus* time curves (Figure 4D). Since mouse liver secretes TG-rich lipoproteins as IDL-like and VLDL particles, we used a solution of 15.3 % NaCl and 35.4 % KBr (final

concentration 0.65 % and 1.52 %, respectively) in saline with a density < 1.019 g/ml to isolate VLDL/IDL. Plasma (0.2 ml) was mixed with 0.8 ml of the NaCl-KBr solution and centrifuged for 100 minutes at 120,000 rpm (627000 g) and 4°C in an ultracentrifuge (rotor TLA 120.2 Beckman). Tubes were sliced at 1.5cm and the top-fraction, containing VLDL/IDL, was collected and frozen at -80°C until composition analyses. VLDL/IDL particle size was determined using a Submicron Particle Sizer (Nicomp, Santa Barbara, CA, USA).

Liver lipid analysis

Liver lipids were extracted according to Bligh & Dyer¹⁹ and determined using commercially available kits. Protein content of tissue homogenates was determined according Lowry *et al.*²⁰

Histology

The localization of hepatic TG and apolipoprotein B (apoB) mRNA were visualized as indicators of TG deposition and VLDL formation, respectively. Hepatic morphology was visualized by standard Hematoxylin Eosin (HE)-staining and neutral lipids were visualized by "Oil-Red-O" (ORO). The apoB *in situ* hybridization technique was similar to that previously described for apoE.²¹ The pGEM-3z vector containing apoB cDNA was a gift from dr. H.M. Princen (Gaubius Laboratory, TNO Prevention and Health, Leiden, The Netherlands).

Mass isotopomer distribution analysis

MIDA allows quantitation of the biosynthesis of polymers *in vivo* and is described in detail elsewhere.²² The enrichment of the pool of acetylCoA precursor units (p) that have entered newly synthesized cholesterol and palmitate during feeding of a [1-¹³C]-acetate-enriched diet can be calculated by comparison with a theoretical table generated using binomial expansion and known isotope frequencies of the atomic isotopes. When the enrichment of the acetylCoA pool is known, it becomes possible to calculate the fraction (f) of newly synthesized cholesterol and palmitate molecules in plasma or tissues. To determine the absolute amount of newly synthesized hepatic cholesterol and palmitate, we multiplied f by the total amount of hepatic free cholesterol and palmitate, respectively. Oral labelling of acetyl-CoA pools with ¹³C-acetate was described by Jung *et al.*²³ By label-feeding for longer periods of time, pools with a slow turnover, such as connective tissue and arterial walls, are also being labelled. After 10 days of labelling, pools with a rapid turnover will have reached a steady state, but pools with a slow turnover might not have. One must realize therefore that this may lead to a certain underestimation in synthesis rates in *ob/ob* mice, mainly for palmitate, since pool sizes of palmitate are larger in these animals.

Gas chromatography/mass spectrometry (GC/MS) analysis

Plasma cholesterol was extracted and derivatized as described.²⁴ Cholesterol-TMS derivatives were separated on a HP 5890 Plus gas chromatograph (Hewlett-Packard, Palo Alto, CA)

Table 1. List of sequences of primers and probes used.

Standard	Type	Sequence	GenBank no.	
<i>β-Actin</i>	Forward	AGC CAT GTA CGT AGC CAT CCA	NM007393	
	Reverse	TCT CCG GAG TCC ATC ACA ATG		
	Probe	TGT CCC TGT ATG CCT CTG GTC GTA CCAC		
Transcription factors				
	<i>Srebp-1c</i>	Forward	GGA GCC ATG GAT TGC ACA TT	BI656094
		Reverse	CCT GTC TCA CCC CCA GCA TA	
Probe		CAG CTC ATC AAC AAC CAA GAC AGT GAC TTC C		
<i>Srebp-2</i>	Forward	CTG CAG CCT CAA GTG CAA AG	AF374267	
	Reverse	CAG TGT GCC ATT GGC TGT CT		
	Probe	CCA TCC AGC AGC AGG TGC AGA CG		
<i>Ppar-α</i>	Forward	TAT TCG GCT GAA GCT GGT GTA C	X57638	
	Reverse	CTG GCA TTT GTT CCG GTT CT		
	Probe	CTG AAT CTT GCA GCT CCG ATC ACA CTT G		
<i>Ppar-γ</i>	Forward	CAC AAT GCC ATC AGG TTT GG	X57638	
	Reverse	GCT GGT CGA TAT CAC TGG AGA TC		
	Probe	CCA ACA GCT TCT CCT TCT CGG CCT G		
<i>Lxr</i>	Forward	GCT CTG CTC ATT GCC ATC AG	AF085745	
	Reverse	TGT TGC AGC CTC TCT ACT TGG A		
	Probe	TCT GCA GAC CGG CCC AAC GTG		
<i>Chrebp</i>	Forward	GAT GGT GCG AAC AGC TCT TCT	AF156604	
	Reverse	CTG GGC TGT GTC ATG GTG AA		
	Probe	CCA GGC TCC TCC TCG GAG CCC		
DNL, cholesterogenesis and β-oxidation				
	<i>Fas</i>	Forward	GGC ATC ATT GGG CAC TCC TT	AF127033
		Reverse	GCT GCA AGC ACA GCC TCT CT	
Probe		CCA TCT GCA TAG CCA CAG GCA ACC TC		
<i>Acc</i>	Forward	GCC ATT GGT ATT GGG GCT TAC	AF374170	
	Reverse	CCC GAC CAA GGA CTT TGT TG		
	Probe	CTC AAC CTG GAT GGT TCT TTG TCC CAG C		
<i>Hmgr</i>	Forward	CCG GCA ACA ACA AGA TCT GTG	BB664708	
	Reverse	ATG TAC AGG ATG GCG ATG CA		
	Probe	TGT CGC TGC TCA GCA CGT CCT CTT C		

Table 1. Continued.

	Type	Sequence	GenBank no.
DNL, cholesterogenesis and β -oxidation	Forward	CTC AGT GGG AGC GAC TCT TCA	AF017175
	Reverse	GGC CTC TGT GGT ACA CGA CAA	
	Probe	CCT GGG GAG GAG ACA GAC ACC ATC CAA C	
<i>Mcad</i>	Forward	GCA GCC AAT GAT GTG TGC TTA C	NM007382
	Reverse	CAC CCT TCT TCT CTG CTT TGG T	
	Probe	CCC TCC GCA GGC TCT GAT GTG G	
<i>Hmgs</i>	Forward	TGG TGG ATG GGA AGC TGT CTA	U12790
	Reverse	TTC TTG CGG TAG GCT GCA TAG	
	Probe	CCA AGG CCC GCA GGT AGC ACT G	
VLDL metabolism	Forward	GCC CAT TGT GGA CAA GTT GAT C	AW012827
	Reverse	CCA GGA CTT GGA GGT CTT GGA	
	Probe	AAG CCA GGG CCT ATC TCC GCA TCC	
<i>Apobec-1</i>	Forward	TCG TCC GAA CAC CAG ATG CT	NM031159
	Reverse	GGT GTC GGC TCA GAA ACT CTG T	
	Probe	CCT GGT TCC TGT CCT GGA GTC CCT G	
<i>ApoE</i>	Forward	CCT GAA CCG CTT CTG GGA TT	NM009696
	Reverse	GCT CTT CCT GGA CCT GGT CA	
	Probe	AAA GCG TCT GCA CCC AGC GCA GG	
<i>Dgat-1</i>	Forward	GGT GCC GTG ACA GAG CAG AT	NM010046
	Reverse	CAG TAA GGC CAC AGC TGC TG	
	Probe	CTG CTG CTA CAT GTG GTT AAC CTG GCC A	
<i>Mttp</i>	Forward	CAA GCT CAC GTA CTC CAC TGA AG	NM008642
	Reverse	TCA TCA TCA CCA TCA GGA TTC CT	
	Probe	ACG GCA AGA CAG CGT GGG CTA CA	
Insulin signaling	Forward	TGA GTC AGC CAG TCT TCG AGA A	NM010568
	Reverse	ACT ACC AGC ATT GGC TGT CCT T	
	Probe	CTG CCA TCA TGT GGT CCH CCT TCT	
<i>Irs-1</i>	Forward	AGC ACC TGG TGG CTC TCT ACA	NM010570
	Reverse	CAG CTG CAG AAG AGC CTG GTA	
	Probe	CTC GCT ATC CGC GGC AAT GGC	
<i>Irs-2</i>	Forward	AGT CCC ACA TCG GGC TTG AAG	AF090738
	Reverse	GGT CTG CAC GGA TGA CCT TAG	
	Probe	CCT TCA AGT CAG CCA GCC CCC TG	

using a 30 m x 0.25 mm (0.2 μ m film thickness) DB5 ms column (J&W Scientific, Folsom, CA, USA) inserted into the ion source of a Quadrupole mass spectrometer, model SSQ 7000 (Finnigan Matt, San Jose, CA, USA). The mass fragments m/z 368, 369, 370 and 371 were monitored by selected ion recording.

For analysis of the methyl esters of palmitate²⁵ the same GC/MS mode described above was used, equipped with a 20 m x 0.18 mm AT1701 column (0.4 μ m film thickness, Alltech Associates Inc, Deerfield, USA). They were analyzed at mass-to-charge ratio (m/z) 271, 272 and 273 (mass isotopomers M_0 , M_1 , and M_2) using chemical ionisation and selected ion recording.

ApoB quantification

ApoB100 concentrations were quantified by comparison to an IDL apoB100 standard isolated from healthy human subjects.²⁶ Since human LDL does not contain apoB48, we were not able to accurately quantify apoB48 levels by this procedure; these levels were estimated. Isolated VLDL samples (10 μ l) were delipidated with methanol and diethylether and dried under nitrogen. Delipidated lipoproteins were reduced in SDS sample buffer (8 M urea, 10 mM Tris base, 2 % SDS, 10 % glycerol, 5 % β -mercaptoethanol) and separated by SDS-PAGE using 4-15 % gradient gels (Ready gels, Biorad, Hercules, CA). Gels were either subjected to silver-staining²⁶ or were used for Western blot analysis. Proteins were transferred onto nitrocellulose membranes (Hybond ECL, Amersham Pharmacia Biotech, Buckinghamshire, UK). Blots were stained with the primary polyclonal antibody against human apolipoprotein B, raised in sheep (dilution 1:100,000; Roche, Mannheim, Germany) and secondary IgG, anti-sheep antibody conjugated with horseradish-peroxidase activity (dilution 1:10,000; Calbiochem, San Diego, CA).

Hepatic gene expression

Total RNA was isolated from ~30 mg tissue using Trizol-methodology (GIBCO, Paisley, UK) followed by the SV Total RNA Isolation System (Promega, Madison, WI). RNA was converted to single-stranded cDNA by a reverse transcription procedure with M-Mulv-RT (Boehringer Mannheim, Mannheim, Germany) and mRNA levels were quantified by real-time PCR using the ABI Prism 7700 Sequence Detection System (Applied Biosystems, Foster City, CA). Procedures were optimized for the particular genes using appropriate forward and reverse primers (GIBCO, Paisley, UK) and a template-specific 3'-TAMRA, 5'-6-FAM labeled Double Dye Oligonucleotide probe (Eurogentec, Seraing, Belgium). Calibration curves were run on serial dilutions of a 8x concentrated cDNA solution, resulting in a series containing 8x, 4x, 2x, 1x, 0.5x, 0.125x, 0.062x, and 0.031x of the cDNA present in the assay incubation. Both assay and calibration incubations were done simultaneously. The fluorescence data obtained were processed using the software program ABI Sequence Detector v1.6.3 (System Applied Biosystems, Foster City, CA). All quantified expression levels were within the linear part of the calibration curves and calculated using these curves. The primers and probe sets used are listed in Table 1.

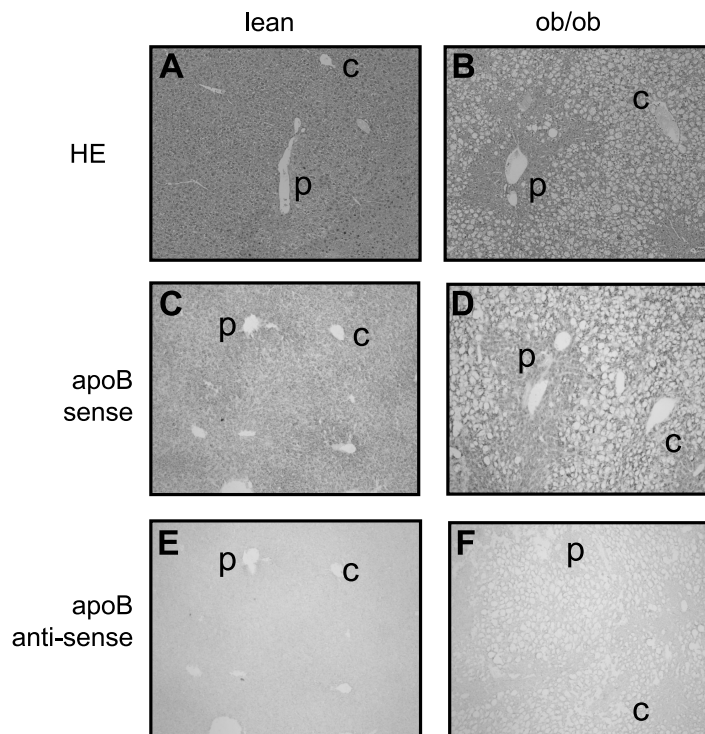
Hepatic insulin signaling

For analysis of IR β and IRS-1,2,3 phosphorylation, liver tissue was homogenized in RIPA - buffer (30 mM Tris, pH 7.5, 1 mM EDTA, 150 mM NaCl, 0.5 % Triton X-100, 0.5 % deoxycholate, 1 mM sodium orthovanadate, 10 mM sodium fluoride, and protease inhibitors (Complete: Boehringer Mannheim)) using a Ultraturrax mixer followed by centrifugation (14 krpm; 15 min; 4°C). Protein content of supernatants was determined using BCA-kit (Pierce, Rockford, IL). A total of 25 μ g protein was analyzed by immunoblotting for expression of IR β subunit (Transduction Laboratories, Lexington), IRS-1,²⁷ IRS-2²⁸ and IRS-3. Anti- IRS3 antibody was obtained from rabbits immunized with a recombinant His-tagged IRS3 fusion protein produced from pET16B-IRS3 (aa198-494 of rat IRS3) as described by Ouwens *et al.*²⁷

Statistical analysis

All values reported are means \pm SD; statistical significance implies $P < 0.05$. Because of small sample sizes, all statistical analyses involved non-parametrical Mann-Whitney U tests.

Figure 1. Hematoxilin Eosin (HE) staining (A, B) and apoB in situ hybridization in liver sections from lean (C, E) and *ob/ob* mice (D, F), respectively. p = portal area (zone 1), c = central area (zone 3).



Results

Animal characteristics

Mean body weight was 26 ± 1 vs. 58 ± 5 g in the lean and *ob/ob* mice, respectively ($P < 0.05$). Fasting plasma glucose, insulin, TG, cholesterol, and FFA concentrations were elevated in *ob/ob* mice (Table 2). Excess TG and cholesterol in *ob/ob* plasma was predominantly found in VLDL-sized fractions upon FPLC separation (data not shown). Liver weight (2-fold), total amount of hepatic TG (5-fold), total cholesterol (~2.6-fold), free cholesterol (~1.6-fold), cholesteryl ester (~15-fold) and glycogen levels (~1.8-fold) were all increased in *ob/ob* mice. No differences in hepatic phospholipid and glucose-6-phosphate (G6P) levels were detected between lean and *ob/ob* mice (Table 2).

Neutral fat deposition (not shown in Figure 1) in *ob/ob* mice was clearly associated with the perivenous (zone 3) area of liver lobules resulting in enlarged, fat-laden hepatocytes in these parts of the liver (Figure 1, A vs. B). To check whether localization of fat in *ob/ob* liver was compatible with that of apolipoprotein B gene expression, *Apob* mRNA was visualized by *in situ* hybridization in lean and *ob/ob* mouse liver (Figure 1, C and D, respectively). *Apob* mRNA was present in the entire liver lobe but a stronger signal was observed in the periportal zone of the liver both in lean and *ob/ob* mice, suggesting zonal differentiation between VLDL formation and TG deposition in *ob/ob* mouse liver.

Table 2. Plasma and hepatic parameters after a 4 hr fast in lean and *ob/ob* mice.

Plasma	Lean	<i>Ob/ob</i>
Glucose (mM)	8.6 ± 3.0	16.9 ± 4.6 *
Insulin (ng/ml)	1.3 ± 0.9	6.9 ± 0.6 *
Triglycerides (mM)	0.3 ± 0.03	0.7 ± 0.1 *
Cholesterol (mM)	1.7 ± 0.4	4.1 ± 0.3 *
Free fatty acids (mM)	0.7 ± 0.1	1.3 ± 0.1 *
Liver		
Liver weight (g)	1.3 ± 0.1	2.7 ± 0.3 *
Triglycerides ($\mu\text{mol/g}$ liver)	1.2 ± 0.4	2.7 ± 0.5 *
Total cholesterol ($\mu\text{mol/g}$ liver)	1.3 ± 0.4	1.6 ± 0.3 *
Free cholesterol ($\mu\text{mol/g}$ liver)	0.8 ± 0.1	1.0 ± 0.1
Cholesteryl esters ($\mu\text{mol/g}$ liver)	0.1 ± 0.01	0.5 ± 0.3 *
Phospholipids ($\mu\text{mol/g}$ liver)	0.3 ± 0.1	0.2 ± 0.3
Glucose-6-phosphate ($\mu\text{mol/g}$ liver)	0.2 ± 0.03	0.1 ± 0.1
Glycogen ($\mu\text{mol/g}$ liver)	212 ± 11	183 ± 17

Data are means \pm SD. $n = 5$ per group. * $P < 0.05$, Mann-Whitney U test.

De novo lipogenesis and cholesterol synthesis

Palmitate and cholesterol synthesis rates in lean and *ob/ob* mice fed an [1-¹³C]-acetate-enriched diet are summarized in Table 3. The enrichment of acetylCoA pool and fractional synthesis rate values could not be calculated in adipose tissue of *ob/ob* mice due to low isotopic enrichments. Enrichments of the hepatic acetylCoA pools for DNL and cholesterol synthesis were similar between lean and *ob/ob* mice. Hepatic fractional *de novo* lipogenesis (DNL) was increased 1.7-fold in *ob/ob* mice in comparison with lean controls. The absolute amount of newly synthesized hepatic palmitate was 10-fold higher in livers of *ob/ob* mice than in those from controls. DNL values in adipose tissue of lean controls indicate that adipocytes may significantly contribute to total DNL in mice. The absolute amounts of newly synthesized cholesterol were similar in livers of both groups.

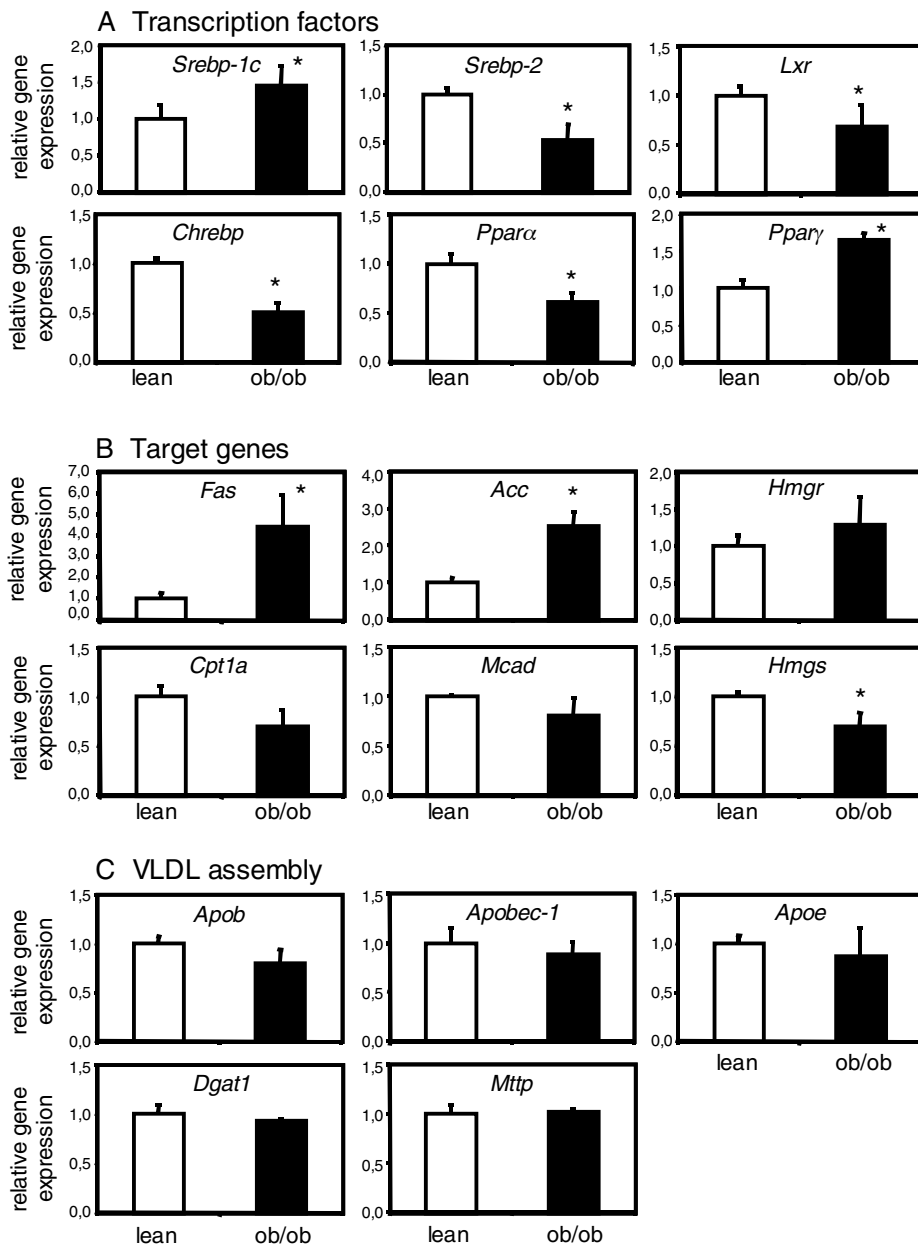
Expression levels of key genes involved in DNL, *i.e.*, fatty acid synthase (*Fas*), and acylCoA carboxylase (*Acc*) were clearly increased in livers of *ob/ob* mice. The mRNA levels of the transcription factor sterol regulatory element binding protein-1c (*Srebp-1c*) was also increased, but gene expression of liver X receptor (*Lxr*) and carbohydrate responsive element-binding protein (*Chrebp*), recently implicated in control of *Fas* expression, were significantly decreased. Expression level of the sterol regulatory binding

Table 3. Acetyl-CoA pool enrichment and fractional palmitate synthesis values of adipose tissue and liver and hepatic acetyl-CoA pool enrichment and fractional cholesterol synthesis values in [1-¹³C]-acetate-enriched diet fed lean and *ob/ob* mice.

	Lean	<i>ob/ob</i>
<i>De novo</i> lipogenesis		
Liver		
Acetyl-CoA pool enrichment (%)	6.3 ± 0.3	5.9 ± 0.8
Fractional hepatic palmitate (%)	31.0 ± 6.1	53.1 ± 4.7 *
Hepatic palmitate (μmol/liver)	1.1 ± 0.4	6.3 ± 0.9 *
Newly synthesized hepatic palmitate (μmol/liver)	0.3 ± 0.1	3.4 ± 0.6 *
Adipose tissue		
Acetyl-CoA pool enrichment (%)	1.6 ± 0.5	ND
Fractional synthesis adipose tissue palmitate (%)	21.5 ± 8.7	ND
Cholesterol synthesis		
Acetyl-CoA pool enrichment (%)	6.3 ± 0.1	5.5 ± 0.5
Fractional synthesis hepatic free cholesterol (%)	17.8 ± 4.0	12.6 ± 3.4 *
Hepatic free cholesterol (μmol/liver)	1.7 ± 0.1	2.7 ± 0.5 *
Newly synthesized hepatic cholesterol (μmol/liver)	0.3 ± 0.1	0.3 ± 0.2

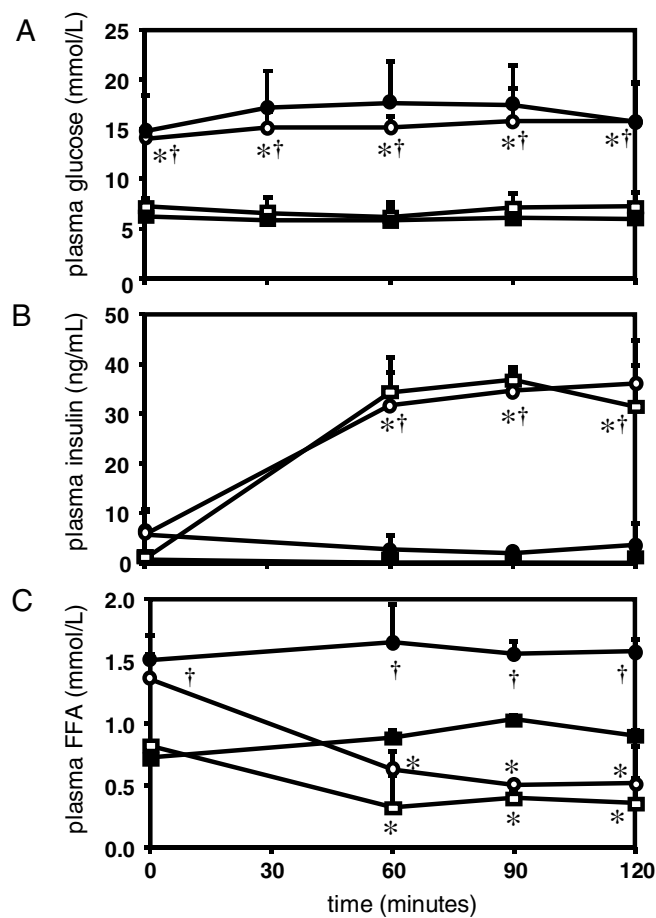
Data are means ± SD. *n* = 5 lean and 5 *ob/ob* mice. * *P* < 0.05, Mann-Whitney U test. ND = not detectable.

Figure 2. Relative hepatic expression levels of several transcription factors (A); their target genes in fatty acid synthesis, cholesterol synthesis and fatty acid oxidation (B); and genes involved in VLDL assembly (C) in lean (white bars) and *ob/ob* mice (black bars). Genes are relative to the hepatic β -Actin expression level. * $P < 0.05$, Mann-Whitney U test.



element protein-2 (*Srebp-2*), involved in control of cellular cholesterol homeostasis, was decreased in *ob/ob* mice liver but this did not result in reduced expression of its target gene HMGCoA reductase (*Hmgr*). Hepatic expression levels of the transcription factor peroxisomal proliferator-activated receptor (*PPAR*)- α was decreased but the expression level of *PPAR*- γ was increased in *ob/ob* mouse liver. Genes involved in ketogenesis and β -oxidation that are controlled by *PPAR* α , *i.e.*, mitochondrial HMG-CoA-synthase (*Hmgs*), carnitine palmitoyl transferase-1a (*Cpt1a*) and medium chain acyl dehydrogenase (*Mcad*), tended to be decreased in *ob/ob* mice, suggesting a decreased β -oxidation in *ob/ob* mouse liver (Figure 2B).

Figure 3. Plasma glucose (A), insulin (B), and FFA (C) levels during a hyperinsulinemic clamp in lean mice receiving saline (closed squares) or insulin (open squares) and in *ob/ob* mice receiving saline (closed circles) or insulin (open circles). $n = 4$ per group. * $P < 0.05$ insulin effect, † $P < 0.05$ mouse strain effect, Mann-Whitney U test.



Hepatic VLDL production under basal conditions and hyperinsulinemic clamp

During the clamp, plasma glucose levels were fixed at fasting (9 h) plasma concentrations that were reached within 60 minutes. Average plasma glucose levels were 7 ± 1 mM and 15 ± 1 mM for lean and *ob/ob* mice, respectively (Figure 3A). Plasma insulin increased to stable levels of 34 ± 3 ng/ml and 34 ± 2 ng/ml in lean and *ob/ob* mice, respectively (Figure 3B). Saline-infused mice maintained their fasting insulin level during the clamp (0.7 ± 0.4 ng/ml and 5 ± 2 ng/ml in lean and *ob/ob* mice, respectively). Plasma FFA levels decreased in the insulin-infused mice only (Figure 3C). Although *ob/ob* mice showed higher basal plasma FFA concentrations, insulin reduced plasma FFA levels to a similar concentration as in lean mice within 60 minutes.

After 60 minutes of saline infusion or hyperinsulinemia, Triton WR1339 was injected to determine VLDL-TG and apoB100 production rates. Basal VLDL-TG production rates were similar in lean and *ob/ob* mice (64 ± 14 and 52 ± 7 $\mu\text{mol/kg/hr}$, respectively, Figure 4A). Acute hyperinsulinemia reduced VLDL-TG production rate to 27 ± 1 $\mu\text{mol/kg/hr}$ (-58 %) in lean mice but only to 41 ± 1 $\mu\text{mol/kg/hr}$ (-21 %) in *ob/ob* mice (Figure 4A). ApoB100 production showed a similar pattern as VLDL-TG production rates. Insulin suppressed apoB100 production much more pronounced in lean mice than in *ob/ob* mice (Figure 4B). The apoB100/B48 ratio in nascent VLDL particles, as determined by intensity scanning of Western blots (Figure 4E), was much higher in *ob/ob* mice than in lean controls: this ratio decreased upon insulin infusion.

Expression of genes encoding apolipoproteins involved in VLDL assembly and secretion, *i.e.*, apoB and apoE, were similar in liver of lean and *ob/ob* mice. In spite of the increased apoB100/B48 ratio in *ob/ob* mouse VLDL, expression of *Apobec-1*, encoding the *Apob* mRNA-editing protein, was not different between both groups indicating a posttranscriptional upregulation of editing activity in *ob/ob* mice. Expression of the genes encoding MTP and DGAT, essential for VLDL lipidation, did not differ between lean and *ob/ob* mice (Figure 2C).

Insulin signaling.

Hepatic mRNA levels of the insulin receptor (*Ir*) and insulin receptor substrate isoforms (*Irs1* and *Irs2*) were decreased in *ob/ob* mice (Figure 5A). Also, phosphorylation of IR β , IRS-1 and IRS-2 proteins was reduced in *ob/ob* mice liver (Figure 5B), indicating decreased hepatic insulin signaling. IRS-3 phosphorylation was slightly increased in the *ob/ob* mouse liver (Figure 5B).

Discussion

The primary defect in the *ob/ob* mouse model is the absence of leptin, resulting in an obese and diabetic phenotype.⁵ The intracellular signal transduction of leptin is similar to that of class 1 cytokine receptors and involves JAK-STAT signaling. Some of these receptors and possibly also leptin signaling can be linked to mitogen-activated protein kinase (MAPK)

Figure 4. VLDL-TG production rate (A), apoB100 production rate (B) and apoB100/B48 band-density-scan-ratio (C) during a hyperinsulinemic clamp in lean and *ob/ob* mice receiving saline (white bars) or insulin (black bars). Triglyceride accumulation curve (D) and a representative Western blot of apoB (E) during hyperinsulinemic clamp in lean and *ob/ob* mice are also shown. $n = 4$ per group. * $P < 0.05$ insulin effect, † $P < 0.05$ mouse strain effect, Mann-Whitney U test.

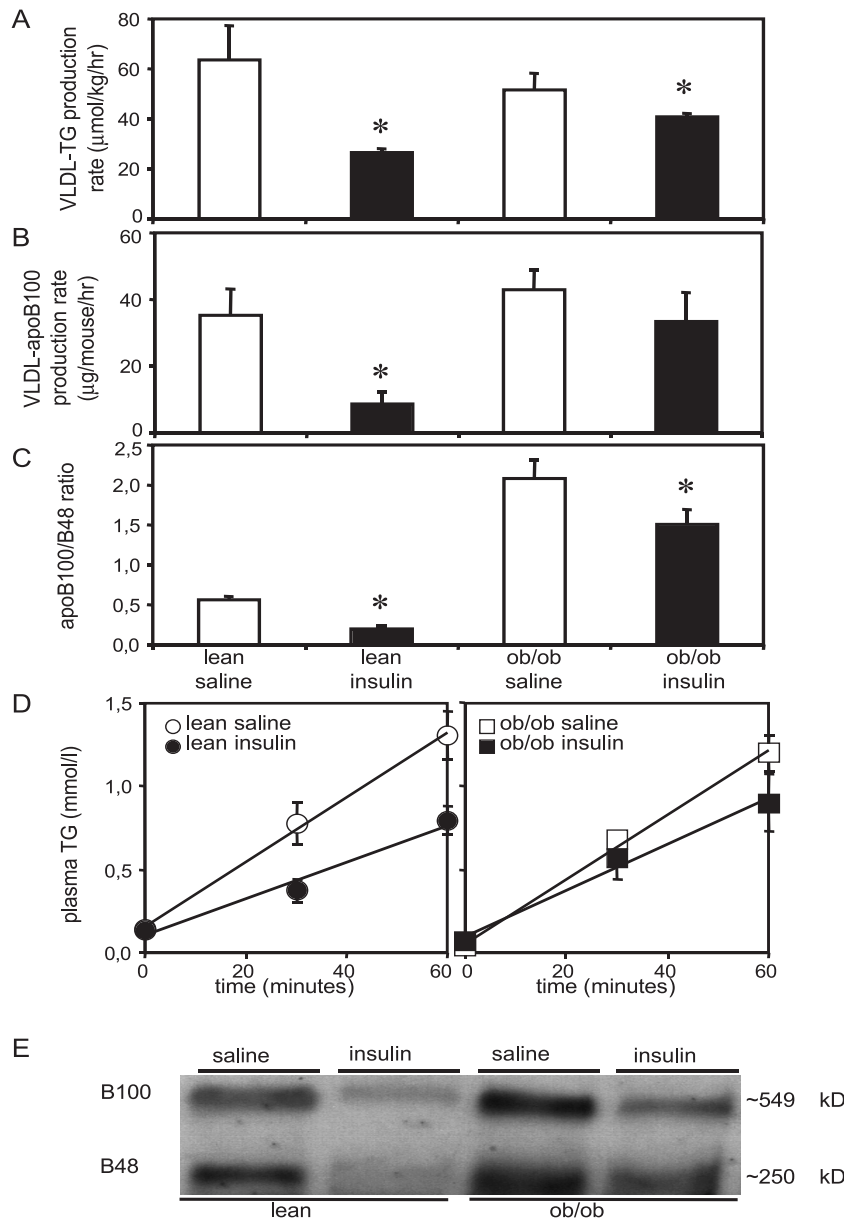
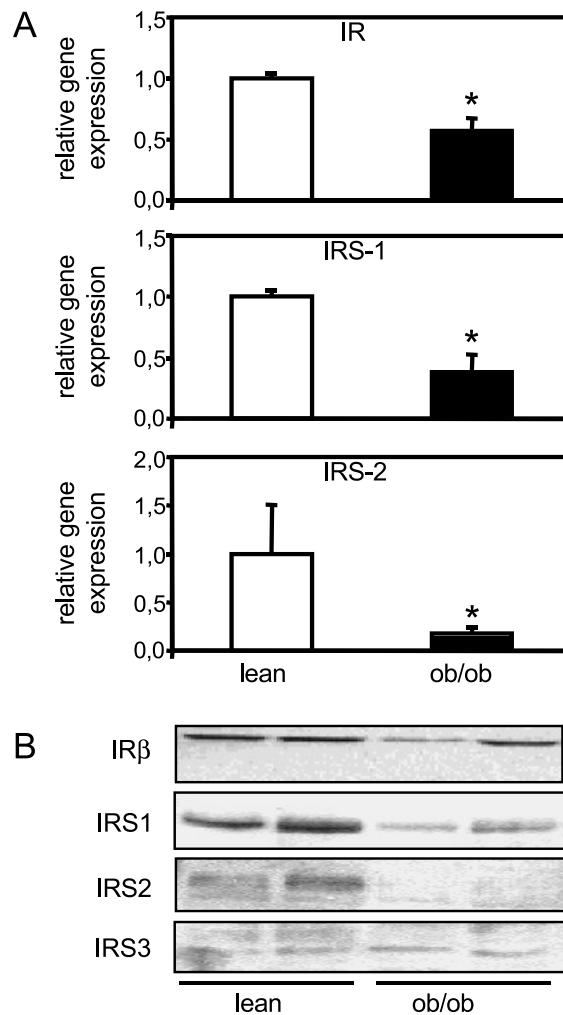


Figure 5. Hepatic gene expression levels (A) and phosphorylation (B) of the insulin receptor (IR) and insulin receptor substrate (IRS)-isoforms in lean and *ob/ob* mice.
* $P < 0.05$, Mann-Whitney U test.



and phosphatidylinositol 3-kinase (PI3K) kinase pathways.^{29,30} However, the metabolic relevance of leptin signaling via these pathways on hepatic fat and cholesterol metabolism and on VLDL production is currently not known. In this study, *ob/ob* mice showed increased plasma FFA levels, a 10-fold increase in hepatic *de novo* lipogenesis (DNL) and a severe, perivenously-localized, hepatic steatosis. Despite these diabetic characteristics, hepatic VLDL production was not increased under fasting conditions, as is the case in humans with insulin resistance or DM2.³¹ The absence of a simultaneous up-

regulation of hepatic cholesterol synthesis, recognized as a crucial factor in control of VLDL production rates,³²⁻³⁴ might contribute to this discordant phenotype. We further demonstrate that the VLDL production process in *ob/ob* mice was insensitive to the suppressive effects of insulin. This disturbance in the control of VLDL production is likely a result of impairment in the transduction pathway(s) of insulin: in livers of *ob/ob* mice IR β , IRS-1 and IRS-2 gene expression levels and protein phosphorylation were clearly decreased. Similar decreases of hepatic and muscle IRS phosphorylation after insulin stimulation *in vivo* were observed in other studies.³⁵⁻³⁷ It is well-established that insulin-mediated suppression of VLDL-apoB secretion in rodent liver cells requires PI3K activation.^{38,39} Phosphatases might play a role in the sequence of events. The phosphotyrosine phosphatase-1B (PTP-1B) has been associated with insulin signaling in different models.^{40,41} Whether this phosphatase is involved in defective insulin signaling in *ob/ob* mouse liver remains to be determined.

Female *ob/ob* mice have been used extensively in metabolic studies concerning hepatic (and muscle) insulin sensitivity.^{8,42} To be able to compare our data with published work we chose to use female *ob/ob* mice for the current experiments. Importantly, studies by Li *et al.* indicate that there are no differences between male and female *ob/ob* mice regarding hepatic lipid deposition or VLDL triglyceride production.^{13,18}

De novo lipogenesis (DNL), suggested as a regulator of VLDL production, was 10-fold increased in *ob/ob* liver. Expression of enzymes involved in lipogenesis are under control of at least three transcription factors, *i.e.*, SREBP-1c, LXR and CHREBP.⁴³⁻⁴⁵ Interestingly, hepatic SREBP-1c expression levels were increased in *ob/ob* mice, whereas those of LXR and CHREBP were decreased, indicating that SREBP-1c is independently able to induce DNL. Since SREBP-1c expression is influenced by insulin⁴⁶ and insulin levels are elevated in *ob/ob* mouse, insulin may continuously induce expression of SREBP-1c and, thereby, of its target genes.⁴³ Thus, insulin resistance may not involve all branches of insulin signaling. Alternatively, leptin has been shown to be able to down-regulate SREBP-1c expression and protein levels and expression of its target gene (*Fas*) in *ob/ob* adipocytes⁴⁷ and in wildtype mouse liver.⁴⁸ IRS2^{-/-} mice, like *ob/ob* mice, have increased hepatic SREBP-1c levels, which normalize upon leptin treatment.⁴⁹ Irrespective of the underlying mechanism, however, our results indicate that upregulated DNL per se is not a regulator of hepatic VLDL production by mouse liver.

In our clamp experiments, plasma insulin levels were similar in both groups. However, both groups were clamped at their basal glucose levels resulting in higher glucose levels in *ob/ob* mice. The question arises to which extent this may have influenced our results with respect to insulin sensitivity of VLDL-TG production. It could be argued that hyperglycemia may directly promote VLDL production. This effect might counteract inhibitory effects of insulin on VLDL-TG secretion. However, in the basal state VLDL production was not increased despite hyperglycemia in *ob/ob* mice, indicating that hyperglycemia is not an independent driving force for VLDL secretion in these animals. Therefore, it is rather unlikely that hyperglycemia per se underlies the profound insulin resistance of VLDL production.

Theoretically, it may be that TG and apoB, required for VLDL assembly, are functionally separated in the *ob/ob* liver. Using *in situ* hybridization, we found that *Apob* mRNA is present in all cells in the liver lobule, but with highest intensity in periportal hepatocytes of control mice. Funahashi *et al.*⁵⁰ reported a uniform distribution of *Apob* mRNA in rat liver, suggesting the existence of species-differences in this respect. In any case, our results suggest that perivenously localized TG in the *ob/ob* mouse liver may be less available for VLDL production.

Substrate availability has been proposed to regulate hepatic VLDL output.³²⁻³⁴ Since the availability of plasma FFA, *de novo* synthesized FA and hepatic TG were all increased in *ob/ob* mice, it is unlikely that the supply of TG is rate-controlling in this respect. The availability of newly synthesized cholesterol may also influence VLDL formation, as has been shown in rats³², rabbits³³, and humans³⁴. Total hepatic cholesterol content in *ob/ob* mouse liver was increased but the absolute cholesterol synthesis rate, as determined by MIDA, was not different from that in lean mice. Cellular cholesterol homeostasis is controlled by SREBP-2. Sterol depletion induces cleavage of membrane-bound SREBP-2, allowing its translocation to the nucleus to induce expression levels of genes involved in cholesterol synthesis and uptake. Increased hepatic cholesterol levels were associated with decreased SREBP-2 expression in *ob/ob* mice, however, this did not lead to alterations in expression levels of HMGCoA reductase (Figure 2) or absolute cholesterol synthesis rates (Table 3). We are aware that our studies were performed under specific experimental conditions. Yet, we tend to hypothesize that limited availability of newly synthesized cholesterol may compromise the ability of the *ob/ob* mouse liver to remove excess TG in the form of VLDL under basal conditions. The resistance of the VLDL assembly/secretion process to the suppressive effects of insulin, however, must result from decreased insulin signaling. According to the current state knowledge,^{38,39} it is highly likely that the PI3K pathway is defective in *ob/ob* mouse liver.

In conclusion, DNL is clearly increased in *ob/ob* mice, probably related to increased SREBP-1c expression levels and despite downregulation of LXR and CHREBP expression. Insufficient supply of newly synthesized cholesterol may become rate-controlling for VLDL production in *ob/ob* mice in a situation in which the supply of FA from plasma and DNL is excessive. Metabolic zonation of TG accumulation and apoB production may contribute in this respect. The inability to induce VLDL-production under these conditions, in combination with impaired hepatic β -oxidation, contributes to development of hepatic steatosis. Insulin signaling is clearly impaired in fatty livers of *ob/ob* mice, resulting in a decreased ability of insulin to suppress VLDL production.

Acknowledgements

This work was supported by the Netherlands Diabetes Foundation (grant 96.604). We thank Vincent Bloks and Juul Baller for their excellent technical assistance.

References

1. Nestel P, Goldrick B. Obesity: changes in lipid metabolism and the role of insulin. *Clin Endocrinol Metab* 1976; 5:313-335.
2. Kissebah AH, Alfarsi S, Evans DJ, Adams PW. Integrated regulation of very low density lipoprotein triglyceride and apolipoprotein-B kinetics in non-insulin-dependent diabetes mellitus. *Diabetes* 1982; 31:217-225.
3. Jungermann K, Kietzmann T. Oxygen: Modulator of metabolic zonation and disease of the liver. *Hepatology* 2000; 31:255-260.
4. Guzman M, Castro J. Zonation of fatty acid metabolism in rat liver. *Biochem J* 1989; 264:107-113.
5. Picard F, Richard D, Huang Q, Deshaies Y. Effects of leptin adipose tissue lipoprotein lipase in the obese *ob/ob* mouse. *Int J Obes Relat Metab Disord* 1998; 22:1088-1095.
6. Shimomura I, Bashmakov Y, Horton JD. Increased levels of nuclear SREBP-1c associated with fatty livers in two mouse models of diabetes mellitus. *J Biol Chem* 1999; 274:30028-30032.
7. Hron WT, Sobocinski KA, Menahan LA. Enzyme activities of hepatic glucose utilization in the fed and fasting genetically obese mouse at 4-5 months of age. *Horm Metab Res Suppl* 1984; 16:32-36.
8. Reul BA, Becker DJ, Ongemba LN, Bailey CJ, Henquin JC, Brichard SM. Improvement of glucose homeostasis and hepatic insulin resistance in *ob/ob* mice given oral molybdate. *J Endocrinol* 1997; 155:55-64.
9. Yen TT, Allan JA, Yu PL, Acton MA, Pearson DV. Triacylglycerol contents and in vivo lipogenesis of *ob/ob*, *db/db* and *Avy/a* mice. *Biochim Biophys Acta* 1976; 441:213-220.
10. Memon RA, Fuller J, Moser AH, Smith PJ, Grunfeld C, Feingold KR. Regulation of putative fatty acid transporters and acyl-CoA synthetase in liver and adipose tissue in *ob/ob* mice. *Diabetes* 1999; 48:121-127.
11. Lewis GF, Uffelman KD, Szeto LW, Steiner G. Effects of acute hyperinsulinemia on VLDL triglyceride and VLDL apoB production in normal weight and obese individuals. *Diabetes* 1993; 42:833-842.
12. Malmstrom R, Packard CJ, Watson TD, Rannikko S, Caslake M, Bedford D, Stewart P, Yki-Jarvinen H, Shepherd J, Taskinen MR. Metabolic basis of hypotriglyceridemic effects of insulin in normal men. *Arterioscler Thromb Vasc Biol* 1997; 17:1454-1465.
13. Li X, Grundy SM, Patel SB. Obesity in *db* and *ob* animals leads to impaired hepatic very low density lipoprotein secretion and differential secretion of apolipoprotein B-48 and B-100. *J Lip Res* 1997; 38:1277-1288.
14. Camus MC, Aubert R, Bourgeois F, Herzog J, Alexiu A, Lemonnier D. Serum lipoprotein and apolipoprotein profiles of the genetically obese *ob/ob* mouse. *Biochim Biophys Acta* 1988; 961:53-64.

15. Bartels ED, Lauritsen M, Nielsen LB. Hepatic expression of microsomal triglyceride transfer protein and in vivo secretion of triglyceride-rich lipoproteins are increased in obese diabetic mice. *Diabetes* 2002; 51:1233-1239.
16. Hawkins M, Barzilai N, Liu R, Chen W, Rossetti L. Role of glucosamine pathway in fat-induced insulin resistance. *J Clin Invest* 1997; 99:2173-2182.
17. Rossetti L, Barzilai N, Chen W, Harris T, Yang D, Rogler CE. Hepatic overexpression of insulin-like growth factor-II in adulthood increases basal and insulin-stimulated glucose disposal in conscious mice. *J Biol Chem* 1996; 271:203-208.
18. Li X, Catalina F, Grundy SM, Patel S. Method to measure apolipoprotein B-48 and B-100 secretion rates in an individual mouse: evidence for a very rapid turnover of VLDL and preferential removal of B-48 relative to B-100-containing lipoproteins. *J Lip Res* 1996; 37:210-220.
19. Bligh EG, Dyer WJ. A rapid method of total lipid extraction and purification. *Can J Biochem Physiol* 1959; 37:911-917.
20. Lowry OH, Rosebrough NJ, Farr AL, Randall RL. Protein measurement with the folin reagents. *J Biol Chem* 1951; 193:265-275.
21. Mensenkamp AR, Teusink B, Baller JF, Wolters H, Havinga R, Van Dijk KW, Havekes LM, Kuipers F. Mice expressing only the mutant APOE3Leiden gene show impaired VLDL secretion. *Arterioscler Thromb Vasc Biol* 2001; 21:1366-1372.
22. Hellerstein MK, Neese RA. Mass isotopomer distribution analysis: a technique for measuring biosynthesis and turnover of polymers. *Am J Physiol* 1992; 263:E988-E1001.
23. Jung HR, Turner SM, Neese RA, Young SG, Hellerstein MK. Metabolic adaptations to dietary fat malabsorption in chylomicron-deficient mice. *Biochem J* 1999; 343: 473-478.
24. Neese RA, Faix D, Kletke C, Wu K, Wang AC, Shackleton CH, Hellerstein MK. Measurement of endogenous synthesis of plasma cholesterol in rats and humans using MIDA. *Am J Physiol* 1993; 264:E136-E147.
25. Lepage G, Roy CC. Direct transesterification of all classes of lipids in a one-step reaction. *J Lipid Res* 1986; 27:114-120.
26. Curtin A, Deegan P, Owens D, Collins P, Johnson A, Tomkin GH. Elevated triglyceride-rich lipoproteins in diabetes. A study of apolipoprotein B-48. *Acta Diabetol* 1996; 33:205-210.
27. Ouwens DM, van der Zon GC, Pronk GJ, Bos JL, Moller W, Cheatham B, Kahn CR, Maassen JA. A mutant insulin receptor induces formation of a Shc-growth factor receptor bound protein 2 (Grb2) complex and p21ras-GTP without detectable interaction of insulin receptor substrate 1 (IRS1) with Grb2. Evidence for IRS1-independent p21ras-GTP formation. *J Biol Chem* 1994; 269:33116-33122.
28. Telting D, van der Zon GC, Dorrestijn J, Maassen JA. IRS-1 tyrosine phosphorylation reflects insulin-induced metabolic and mitogenic responses in 3T3-L1 pre-adipocytes. *Arch Physiol Biochem* 2001; 109:52-62.
29. Bjorbaek C, Uotani S, da Silva B, Flier JS. Divergent signaling capacities of the long and short isoforms of the leptin receptor. *J Biol Chem* 1997; 272:32686-32695.

30. Kellerer M, Koch M, Metzinger E, Mushack J, Capp E, Haring HU. Leptin activates PI-3 kinase in C2C12 myotubes via janus kinase-2 (JAK-2) and insulin receptor substrate-2 (IRS-2) dependent pathway. *Diabetologia* 1997; 40:1358-1362.
31. Malmstrom R, Packard CJ, Caslake M, Bedford D, Stewart P, Yki-Jarvinen H, Shepherd J, Taskinen MR. Defective regulation of triglyceride metabolism by insulin in the liver in NIDDM. *Diabetologia* 1997; 40:454-462.
32. Khan B, Wilcox HG, Heimberg M. Cholesterol is required for secretion of very-low-density lipoprotein by rat liver. *Biochem J* 1989; 258:807-816.
33. Mackinnon AM, Savage J, Gibson RA, Barter PJ. Secretion of cholesteryl ester-enriched very low density lipoproteins by the liver of cholesterol-fed rabbits. *Atherosclerosis* 1985; 54:145-155.
34. Watts GF, Naoumova R, Cummings MH, Umpleby AM, Slavin BM, Sonksen PH, Thompson GR. Direct correlation between cholesterol synthesis and hepatic secretion of apolipoprotein B-100 in normolipidemic subjects. *Metabolism* 1995; 44:1052-1057.
35. Saad MJA, Araki E, Miralpeix M, Rothenberg PL, White MF, Kahn CR. Regulation of insulin receptor substrate-1 in liver and muscle of animal models of insulin resistance. *J Clin Invest* 1992; 90:1839-1849.
36. Kerouz NJ, Horsch D, Pons S, Kahn CR. Differential regulation of insulin receptor substrates-1 and -2 (IRS-1 and IRS-2) and phosphatidylinositol 3-kinase isoforms in liver and muscle of the obese diabetic (*ob/ob*) mouse. *J Clin Invest* 1997; 100:3164-3172.
37. Shimomura I, Matsuda M, Hammer RE, Bashmakov Y, Brown MS, Goldstein JL. Decreased IRS-2 and increased SREBP-1c lead to mixed insulin resistance and sensitivity in livers of lipodystrophic and *ob/ob* mice. *Mol Cell* 2000; 6:77-86.
38. Sparks JD, Phung TL, Bolognini M, Sparks C. Insulin-mediated inhibition of apolipoprotein B secretion requires an intracellular trafficking event and phosphatidylinositol 3-kinase activation: studies with Brefeldin A and Wortmannin in primary cultures of rat hepatocytes. *Biochem J* 1996; 313:567-574.
39. Phung TL, Roncone A, de Mesy Jensen KL, Sparks CE, Sparks JD. Phosphoinositide 3-kinase activity is necessary for insulin-dependent inhibition of apolipoprotein B secretion by rat hepatocytes and localizes to the endoplasmic reticulum. *J Biol Chem* 1997; 272:30693-30702.
40. Elchebly M, Payette P, Michaliszyn E, Cromlish W, Collins S, Loy AL, Normandin D, Cheng A, Himms-Hagen J, Ramachandran C, Gresser MJ, Tremblay MI, Kennedy HP. Increased insulin sensitivity and obesity resistance in mice lacking the protein tyrosine phosphatase-1B gene. *Science* 1999; 283:1423-1425.
41. Taghibiglou C, Rashid-Kolvear R, Van Iderstine SC, Le-Tien H, Fantus IG, Lewis GF, Adeli K. Hepatic very low density lipoprotein-ApoB overproduction is associated with attenuated hepatic insulin signaling and overexpression of protein-tyrosine phosphatase 1 B in a fructose-fed hamster model of insulin resistance. *J Biol Chem* 2002; 277:793-803.

42. Harris RB. Parabiosis between db/db and ob/ob or db/+ mice. *Endocrinology* 1999; 140:138-145.
43. Koo S-H, Dutcher AK, Towle HC. Glucose and insulin function through two distinct transcription factors to stimulate expression of lipogenic enzyme genes in liver. *J Biol Chem* 2001; 276:9437-9445.
44. Yamashita H, Takenoshita M, Sakurai M, Bruick RK, Henzel WJ, Shillinglaw W, Arnot D, Uyeda K. A glucose-responsive transcription factor that regulates carbohydrate metabolism in the liver. *PNAS* 2001; 98:9116-9121.
45. Kawaguchi T, Osatomi K, Yamashita H, Kabashima T, Uyeda K. Mechanism for fatty acid "sparing" effect on glucose-induced transcription: regulation of carbohydrate-responsive element-binding protein by AMP-activated protein kinase. *J Biol Chem* 2002; 277:3829-3835.
46. Foretz M, Guichard C, Ferre P, Foufelle F. Sterol regulatory element binding protein-1c is a major mediator of insulin action on the hepatic expression of glucokinase and lipogenesis-related genes. *PNAS* 1999; 96:12737-12742.
47. Soukas A, Cohen P, Succi ND, Friedman JM. Leptin-specific patterns of gene expression in white adipose tissue. *Genes Dev* 2000; 14:963-980.
48. Kakuma T, Lee Y, Higa M, Wang Z-W, Pan W, Shimomura I, Unger RH. Leptin, troglitazone, and the expression of sterol regulatory element binding proteins in liver and pancreatic islets. *PNAS* 2000; 97:8536-8541.
49. Tobe K, Suzuki R, Aoyama M, Yamauchi T, Kamon J, Kubota N, Tereuchi Y, Matsui J, Akanuma Y, Kimura S, Tanaka J, Abe M, Ohsumi J, Nogai R, Kadowaki T. Increased expression of the sterol regulatory element binding protein-1 gene in insulin receptor substrate-2 (-/-) mouse liver. *J Biol Chem* 2001; 276:38337-38340.
50. Funahashi T, Giannoni F, DePaoli AM, Skarosi SF, Davidson NO. Tissue-specific, developmental and nutritional regulation of the gene encoding the catalytic subunit of the rat apolipoprotein B mRNA editing enzyme: functional role in the modulation of apoB mRNA editing. *J Lipid Res* 1995; 36:414-428.